

Anisotropic Keldysh interaction

Andrei Galiautdinov

*Department of Physics and Astronomy, University of Georgia, Athens, Georgia 30602, USA**

(Dated: July 2, 2019)

We generalize the classic calculations by Rytova and Keldysh of screened Coulomb interaction in semiconductor thin films to systems with anisotropic permittivity tensor. Explicit asymptotic expressions for electrostatic potential energy of interaction in the weakly anisotropic case are found in closed analytical form. The case of strong in-plane anisotropy, however, requires evaluation of the inverse Fourier transform of $1/(k + Ak_x^2 + Bk_y^2)$, which, at present, remains unresolved.

Keywords: semiconductor films; dielectric screening; Keldysh interaction; anisotropy

I. INTRODUCTION

The important role played by the dielectric screening in determining excitonic properties of various two-dimensional semiconductor heterostructures has been the subject of numerous investigations over the last several decades (for recent studies see, for example, [1–13]). A particularly interesting direction of current experimental research involves perovskite chalcogenide films whose in-plane dielectric anisotropy gives rise to some rather unusual optical behavior [14, 15]. Past theoretical work on two-dimensional dielectric screening involved various *ab initio* calculations [1, 2], the use of the nonlinear Thomas-Fermi model [4], [7], the modified Mott-Wannier approach [8], the transfer matrix method [13], as well as various approaches based on effective mass approximation [6, 10]. Here we pursue what is likely the simplest possibility — generalization to anisotropic films of classic calculations by Rytova [16] and Keldysh [17, 18]. The motivation for this approach is rather obvious: we want to get a better sense of how the famous *isotropic* form of screened electrostatic interaction energy,

$$V(\rho) = (\pi qq' / \epsilon d) [H_0(\rho/\rho_0) - Y_0(\rho/\rho_0)], \quad (1)$$

is modified under the minimal number of microscopic assumptions. In what follows, we provide the general expression for the Fourier image of the anisotropic potential in momentum space, and analytically work out in real space the *weakly* anisotropic case only. Interested readers are invited to improve on that calculation by exploring the *strongly* anisotropic scenario.

II. GENERAL CONSIDERATIONS

The electrostatic potential energy of interaction between charges q and q' located at $(\boldsymbol{\rho}, z)$ and $(\mathbf{0}, z')$ ($z > z'$, $\boldsymbol{\rho} = (x, y)$) inside an *anisotropic* semiconductor film of thickness d surrounded by two isotropic media with dielectric constants ϵ_1 and ϵ_2 is given by (see Appendix for derivation and Fig. 6; compare with [16, 17])

$$V(\boldsymbol{\rho}, z, z') = \int \frac{d^2 \mathbf{k}}{(2\pi)^2} e^{i\mathbf{k} \cdot \boldsymbol{\rho}} V(\mathbf{k}, z, z'), \quad (2)$$

with

$$V(\mathbf{k}, z, z') = \frac{4\pi qq'}{\epsilon_z} \frac{\cosh \left[\tilde{k} \left(\frac{d}{2} - z \right) + \tilde{\eta}_2 \right] \cosh \left[\tilde{k} \left(\frac{d}{2} + z' \right) + \tilde{\eta}_1 \right]}{\tilde{k} \sinh[\tilde{k}d + \tilde{\eta}_1 + \tilde{\eta}_2]}, \quad (3)$$

where

$$\tilde{\eta}_{1,2} = \frac{1}{2} \ln \left(\frac{\epsilon_z \tilde{k} + \epsilon_{1,2} k}{\epsilon_z \tilde{k} - \epsilon_{1,2} k} \right), \quad \tilde{k} = \sqrt{\frac{\epsilon_x k_x^2 + \epsilon_y k_y^2}{\epsilon_z}}, \quad k = \sqrt{k_x^2 + k_y^2}, \quad (4)$$

*Electronic address: ag@physast.uga.edu

and the axes of the coordinate system (x, y, z) coincide with the principal axes of the film's permittivity tensor, $\epsilon = \text{diag}(\epsilon_x, \epsilon_y, \epsilon_z)$. In the most interesting for practical applications scenario, $\epsilon_{1,2} \ll \epsilon_x, \epsilon_y, \epsilon_z$, and, for distances $\rho \gg |z - z'| \sim d$, the main contribution to the integral in (2) comes from \mathbf{k} satisfying $kd \ll k\rho \lesssim 1$. Under these conditions, $\tilde{k}d \ll 1$, $\tilde{\eta}_{1,2} \approx \epsilon_{1,2}k/(\epsilon_z \tilde{k})$, and, with the dependence on z and z' disappearing, we get the two-dimensional form of the interaction,

$$V(\boldsymbol{\rho}) = \frac{4\pi qq'}{(2\pi)^2 d} \int \frac{d^2 \mathbf{k} e^{i\mathbf{k} \cdot \boldsymbol{\rho}}}{\epsilon_x k_x^2 + \epsilon_y k_y^2 + (\epsilon_1 + \epsilon_2) \frac{k}{d}}. \quad (5)$$

At this point it is convenient to introduce two ‘‘screening’’ lengths,

$$\rho_{0x} \equiv \frac{\epsilon_x d}{\epsilon_1 + \epsilon_2}, \quad \rho_{0y} \equiv \frac{\epsilon_y d}{\epsilon_1 + \epsilon_2}, \quad (6)$$

characterizing polarizability of the film in the x and y directions, respectively, and write the interaction (5) in the form

$$V(\boldsymbol{\rho}) = \frac{qq'}{\pi(\epsilon_1 + \epsilon_2)} \int \frac{d^2 \mathbf{k} e^{i\mathbf{k} \cdot \boldsymbol{\rho}}}{k \epsilon(\mathbf{k})}, \quad (7)$$

where $\epsilon(\mathbf{k})$ is the dielectric function, formally defined by

$$\epsilon(\mathbf{k}) = 1 + \frac{1}{k} (\rho_{0x} k_x^2 + \rho_{0y} k_y^2), \quad (8)$$

which generalizes the standard isotropic result [2]. In Ref. [19], for the case of surrounding vacuum in the *isotropic* scenario, the authors have numerically verified that the screening length of a monolayer can be calculated with good accuracy on the basis of Eq. (6) provided the dielectric contrast is large and the relevant dielectric constant of the monolayer is the in-plane component of the permittivity tensor of the bulk material. We take that as an indication that the Keldysh model is a good approximation to realistic experimental situations and hypothesize that its anisotropic generalization proposed here should work reasonably well even for samples of monolayer thickness.

The problem thus reduces to the calculation of a two-dimensional Fourier integral,

$$F(x, y) = \int \frac{dk_x dk_y}{(2\pi)^2} \frac{e^{i(k_x x + k_y y)}}{k + Ak_x^2 + Bk_y^2}, \quad (9)$$

with $A, B > 0$. To that end, working in polar coordinates, we write,

$$\begin{aligned} V(\boldsymbol{\rho}) &= \frac{qq'}{\pi(\epsilon_1 + \epsilon_2)} \int_0^\infty \int_0^{2\pi} \frac{dt d\theta e^{it \cos \theta}}{t[\rho_{0x} \cos^2(\theta + \alpha) + \rho_{0y} \sin^2(\theta + \alpha)] + \rho} \\ &= \frac{2qq'}{(\epsilon_1 + \epsilon_2)\rho_0} \int_0^\infty dt \frac{I(t, \alpha, a, b)}{t + b}, \end{aligned} \quad (10)$$

where $t = k\rho$, α is the angle between the position vector $\boldsymbol{\rho}$ and the positive x -axis, as shown in Fig. 6,

$$I(t, \alpha, a, b) = \frac{1}{2\pi} \int_0^{2\pi} d\theta \frac{e^{it \cos \theta}}{1 - \varepsilon^2(t, a, b) \cos^2(\theta + \alpha)}, \quad (11)$$

and

$$\varepsilon^2(t, a, b) \equiv \frac{at}{t + b}, \quad a \equiv 1 - \frac{\rho_{0x}}{\rho_{0y}}, \quad b \equiv \frac{\rho}{\rho_0}, \quad \rho_0 \equiv \rho_{0y}, \quad (12)$$

with $a \in (-\infty, 1]$ playing the role of the anisotropy parameter; the greater the $|a|$, the greater the anisotropy, with $a = 0$ corresponding to the isotropic case.

Without loss of generality, we may assume that $0 < \rho_{0x} \leq \rho_{0y}$, and thus $0 \leq a < 1$. Then, since $t \geq 0$, we have $0 \leq \varepsilon^2(t) < 1$. Taking into account the well-known Fourier series expansion [20],

$$\frac{1}{1 - \varepsilon^2 \cos^2 \chi} = \frac{1}{\sqrt{1 - \varepsilon^2}} \left[1 + 2 \sum_{n=1}^{\infty} \left(\frac{\varepsilon}{1 + \sqrt{1 - \varepsilon^2}} \right)^{2n} \cos(2n\chi) \right], \quad (13)$$

and using the fact that $\int_0^{2\pi} d\theta e^{it \cos \theta} \sin(2n\theta) = 0$, we get for the θ -integral in (11) the asymptotic multipole series,

$$\begin{aligned}
I(t, \alpha, a, b) &= \frac{1}{\sqrt{1-\varepsilon^2(t)}} \frac{1}{2\pi} \int_0^{2\pi} d\theta e^{it \cos \theta} \\
&+ \frac{2}{\sqrt{1-\varepsilon^2(t)}} \sum_{n=1}^{\infty} \left(\frac{\varepsilon(t)}{1+\sqrt{1-\varepsilon^2(t)}} \right)^{2n} \left(\frac{1}{2\pi} \int_0^{2\pi} d\theta e^{it \cos \theta} \cos(2n\theta) \right) \cos(2n\alpha) \\
&= \frac{J_0(t)}{\sqrt{1-\varepsilon^2(t)}} \\
&+ \frac{2}{\sqrt{1-\varepsilon^2(t)}} \left(\frac{\varepsilon(t)}{1+\sqrt{1-\varepsilon^2(t)}} \right)^2 \frac{tJ_0(t) - 2J_1(t)}{t} \cos(2\alpha) \\
&+ \frac{2}{\sqrt{1-\varepsilon^2(t)}} \left(\frac{\varepsilon(t)}{1+\sqrt{1-\varepsilon^2(t)}} \right)^4 \frac{t(t^2 - 24)J_0(t) - 8(t^2 - 6)J_1(t)}{t^3} \cos(4\alpha) \\
&+ \frac{2}{\sqrt{1-\varepsilon^2(t)}} \left(\frac{\varepsilon(t)}{1+\sqrt{1-\varepsilon^2(t)}} \right)^6 \frac{t(t^4 - 144t^2 + 1920)J_0(t) - 6(3t^4 - 128t^2 + 640)J_1(t)}{t^5} \cos(6\alpha) + \dots,
\end{aligned} \tag{14}$$

where J_0 and J_1 are the Bessel functions of the first kind.

III. WEAK ANISOTROPY

In a rather straightforward manner (for a better approach see Sec. IV), assuming $0 \leq a \ll 1$ and treating $\varepsilon^2(t, a, b)$ as a small parameter in (14), we get, in lowest order,

$$I(t) \approx J_0(t) + \frac{\varepsilon^2(t)}{2} J_0 + \frac{\varepsilon^2(t)}{2} \left(J_0(t) - \frac{2J_1(t)}{t} \right) \cos(2\alpha), \tag{15}$$

and, thus,

$$V(b, \alpha) = \frac{2qq'}{(\varepsilon_1 + \varepsilon_2)\rho_0} \int_0^\infty dt \left\{ \frac{J_0(t)}{t+b} + \frac{a}{2} \left[\frac{tJ_0(t)}{(t+b)^2} + \frac{tJ_0(t) - 2J_1(t)}{(t+b)^2} \cos(2\alpha) \right] \right\}. \tag{16}$$

Performing the remaining t -integration we find,

$$V(b, \alpha) = V_0(b) + V_1(b, \alpha), \tag{17}$$

where

$$V_0(b, \alpha) = \frac{\pi qq'}{(\varepsilon_1 + \varepsilon_2)\rho_0} [H_0(b) - Y_0(b)] \tag{18}$$

is the standard Keldysh-Rytova result, and

$$\begin{aligned}
V_1(b, \alpha) &= \frac{a}{2} \frac{\pi qq'}{(\varepsilon_1 + \varepsilon_2)\rho_0} \left[H_0(b) - Y_0(b) + \frac{2}{\pi} b + bY_1(b) - bH_1(b) \right] \\
&+ \frac{a}{2} \frac{\pi qq'}{(\varepsilon_1 + \varepsilon_2)\rho_0} \left[\frac{2}{\pi} b^3 + b[(b^2 - 2)Y_1(b) + bY_0(b)] - b[(b^2 - 2)H_1(b) + bH_0(b)] - \frac{4}{\pi} \right] \frac{\cos(2\alpha)}{b^2}
\end{aligned} \tag{19}$$

is the linear correction whose graph is shown in Fig. 1 (assuming $qq' < 0$). In the above, various H_i and Y_i denote the Struve and Neumann functions, respectively.

For $b \ll 1$, or $d \ll \rho \ll \rho_0$, we get

$$V_0 = \frac{2qq'}{(\varepsilon_1 + \varepsilon_2)\rho_0} \left[\ln \left(\frac{2}{b} \right) - \gamma \right] = \frac{2qq'}{(\varepsilon_1 + \varepsilon_2)\rho_0} \left[\ln \left(\frac{2\rho_0}{\rho} \right) - \gamma \right], \tag{20}$$

$$V_1 = \frac{aqq'}{(\varepsilon_1 + \varepsilon_2)\rho_0} \left[\ln \left(\frac{2}{b} \right) - \gamma - 1 - \frac{\cos(2\alpha)}{2} \right] = \frac{aqq'}{(\varepsilon_1 + \varepsilon_2)\rho_0} \left[\ln \left(\frac{2\rho_0}{\rho} \right) - \gamma - 1 - \frac{\cos(2\alpha)}{2} \right], \tag{21}$$

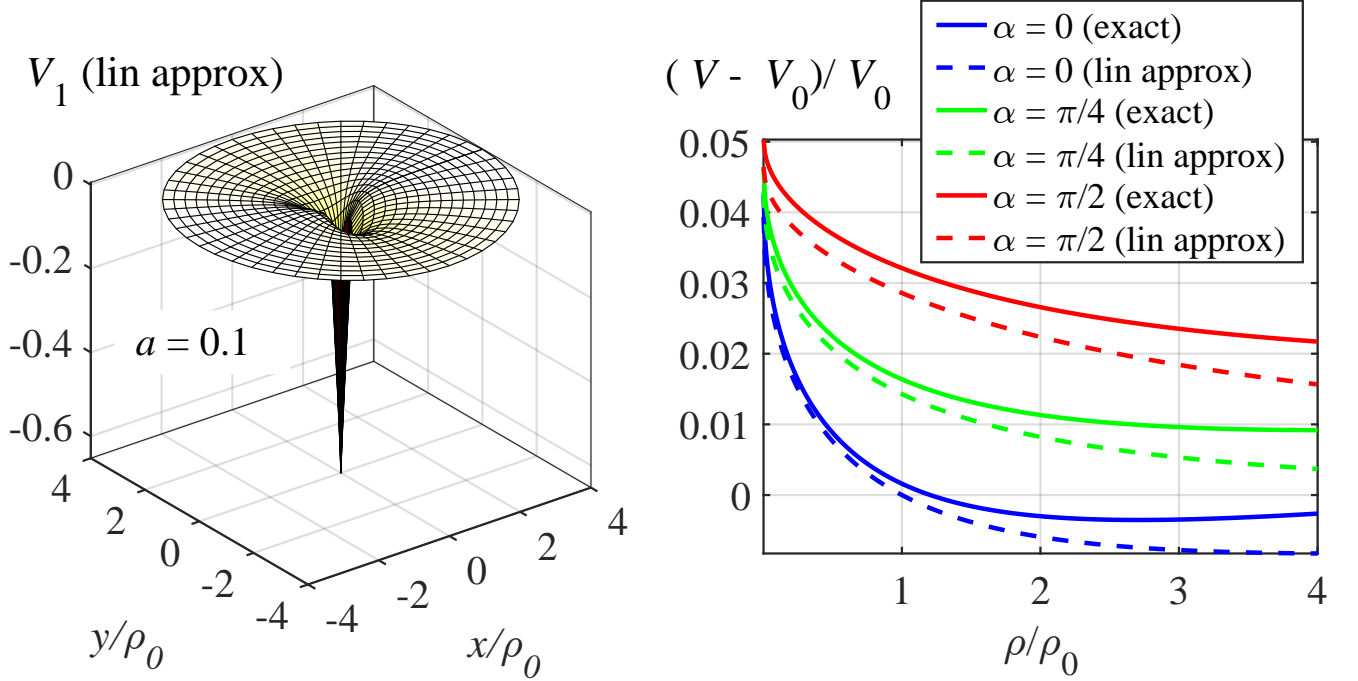


FIG. 1: Graphs of V_1 in units of $|qq'|/(\epsilon_1 + \epsilon_2)\rho_0$, and V_1/V_0 , with $a = 0.1$, in the weakly anisotropic case, calculated on the basis of Eqs. (19) and (18) and direct numerical integration in Eq. (10).

where $\gamma \approx 0.577216$ is the Euler constant. Since $\int_0^{2\pi} \cos(2\alpha) d\alpha = 0$, the excitonic ground state energy in this case experiences a first order shift,

$$\Delta E_0 = \frac{2\pi a q q'}{(\epsilon_1 + \epsilon_2)\rho_0} \int_0^\infty \left(\ln\left(\frac{2}{b}\right) - \gamma - 1 \right) |\psi_0(b)|^2 b db, \quad (22)$$

where $\psi_0(b)$ is the unperturbed axially symmetric ground state wave function. On the other hand, for $b \gg 1$, or $\rho \gg \rho_0$, Eqs. (18) and (19) reproduce the standard Coulomb asymptotics,

$$V(\rho) = \frac{2q q'}{(\epsilon_1 + \epsilon_2)\rho_0} \left(\frac{1}{b} - \frac{a \cos(2\alpha)}{b^2} \right) \rightarrow \frac{2q q'}{(\epsilon_1 + \epsilon_2)\rho}. \quad (23)$$

To get a sense of the error involved in this linear approximation, we define two relative errors by

$$\text{Err}_1 \equiv \frac{V_{\text{exact}} - V_{\text{approx}}}{V_{\text{exact}}} = \frac{V_{1\text{exact}} - V_1}{V_{\text{exact}}} \quad (24)$$

and

$$\text{Err}_2 \equiv \frac{V_{\text{exact}} - V_{\text{approx}}}{V_{\text{exact}} - V_0} = \frac{V_{1\text{exact}} - V_1}{V_{1\text{exact}}}, \quad (25)$$

respectively, with $V_{1\text{exact}} \equiv V_{\text{exact}} - V_0$. Here, $V_{\text{approx}} \equiv V_0 + V_1$ is calculated on the basis of Eqs. (18) and (19), and V_{exact} is found by direct numerical integration of the double integral in (10). The corresponding results are summarized in Fig. 2. Notice that for all ρ the error Err_1 is greatest for points with $\alpha = \pi/2$. The error Err_2 is particularly troublesome, as the blue curve clearly indicates.

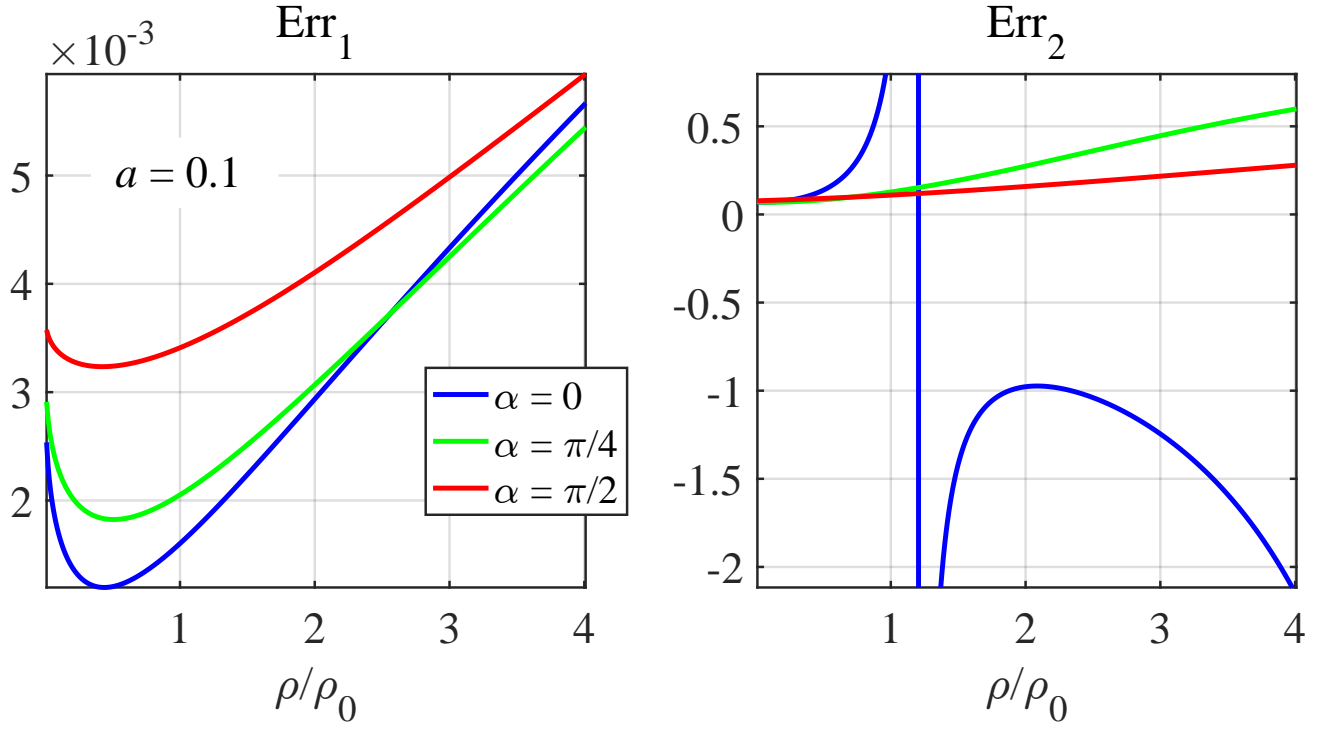


FIG. 2: Graphs of the relative errors defined in Eqs. (24) and (25). The vertical asymptote (in blue) is at the point with $\alpha = 0$, for which $V = V_0$ (exact Keldysh value); compare with Fig. 1.

IV. WEAK ANISOTROPY: RENORMALIZED KELDYSH INTERACTION

A better linear approximation can be achieved by “renormalizing” the zeroth order Keldysh contribution, V_0 , as follows: we re-write the monopole term in (14) as shown below,

$$I = \frac{J_0(t)}{\sqrt{1-a}} + \underbrace{\left[\left(\frac{J_0(t)}{\sqrt{1-\varepsilon^2(t)}} - \frac{J_0(t)}{\sqrt{1-a}} \right) + \frac{2}{\sqrt{1-\varepsilon^2(t)}} \left(\frac{\varepsilon(t)}{1+\sqrt{1-\varepsilon^2(t)}} \right)^2 \frac{tJ_0(t) - 2J_1(t)}{t} \cos(2\alpha) + \dots \right]}_{\sim \mathcal{O}(a)}, \quad (26)$$

and expand everything in square brackets to linear (leading!) order in a . The potential then becomes

$$V(b, \alpha) = \frac{2qq'}{(\epsilon_1 + \epsilon_2)\rho_0} \int_0^\infty dt \left\{ \frac{1}{\sqrt{1-a}} \frac{J_0(t)}{t+b} + \frac{a}{2} \left[-\frac{bJ_0(t)}{(t+b)^2} + \frac{tJ_0(t) - 2J_1(t)}{(t+b)^2} \cos(2\alpha) \right] \right\}, \quad (27)$$

which should be compared with (16). We then find

$$V(b, \alpha) = V_{0\text{ren}} + V_{1\text{ren}}, \quad (28)$$

where

$$V_{0\text{ren}}(b, \alpha) = \frac{\pi qq'}{(\epsilon_1 + \epsilon_2)\rho_0} \frac{H_0(b) - Y_0(b)}{\sqrt{1-a}} \quad (29)$$

is the *renormalized* isotropic Keldysh term, and

$$V_{1\text{ren}}(b, \alpha) = \frac{a}{2} \frac{\pi qq'}{(\epsilon_1 + \epsilon_2)\rho_0} \left[\frac{2}{\pi} b + bY_1(b) - bH_1(b) \right] + \frac{a}{2} \frac{\pi qq'}{(\epsilon_1 + \epsilon_2)\rho_0} \left[\frac{2}{\pi} b^3 + b[(b^2 - 2)Y_1(b) + bY_0(b)] - b[(b^2 - 2)H_1(b) + bH_0(b)] - \frac{4}{\pi} \right] \frac{\cos(2\alpha)}{b^2} \quad (30)$$

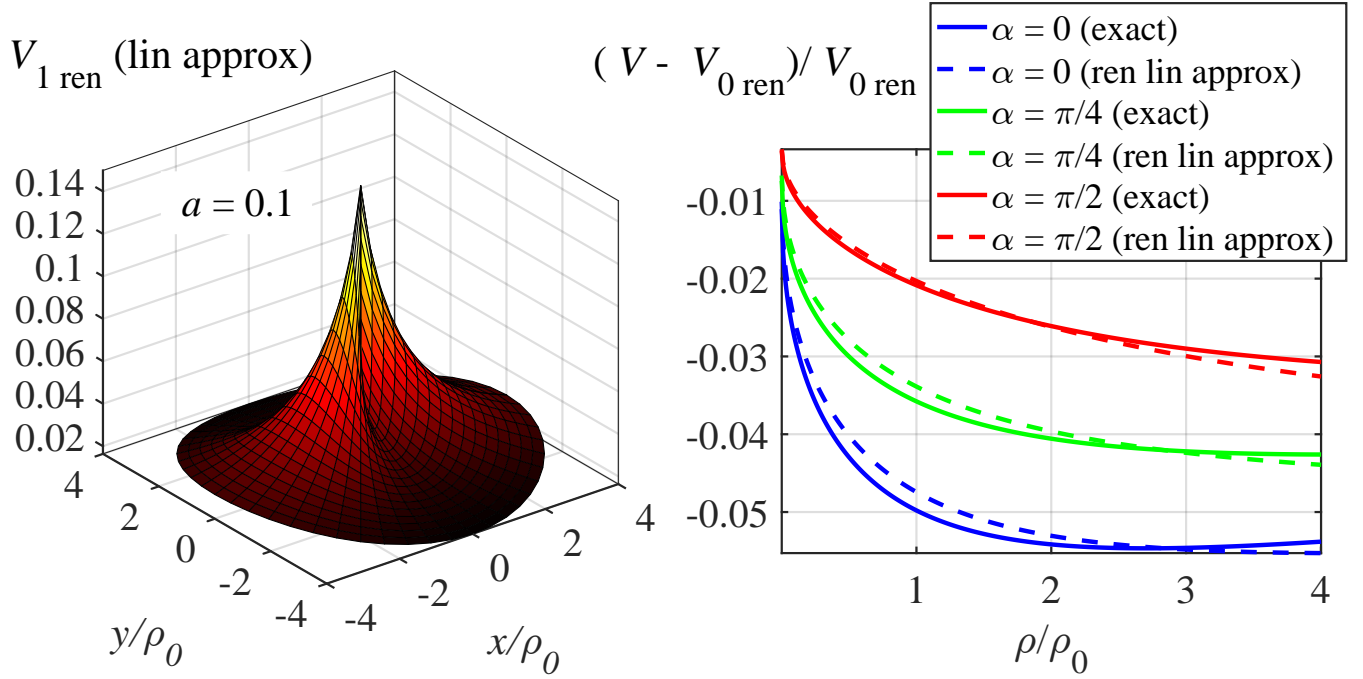


FIG. 3: Graphs of $V_{1\text{ren}}$ in units of $|qq'|/(\epsilon_1 + \epsilon_2)\rho_0$, and $V_{1\text{ren}}/V_{0\text{ren}}$, with $a = 0.1$, in the weakly anisotropic case, calculated on the basis of Eqs. (29) and (30) and direct numerical integration in Eq. (10). Compare with Fig. 1.

is the corresponding linear correction consisting of a linear monopole and a linear dipole contributions, Fig. 3. Now in the $b \ll 1$ limit we get

$$V_{0\text{ren}} = \frac{2qq'}{(\epsilon_1 + \epsilon_2)\rho_0} \frac{\ln\left(\frac{2}{b}\right) - \gamma}{\sqrt{1-a}} \quad (31)$$

and a perfectly reasonable first order correction

$$V_{1\text{ren}} = -\frac{aqq'}{(\epsilon_1 + \epsilon_2)\rho_0} \left[1 + \frac{\cos(2\alpha)}{2} \right], \quad (32)$$

which does not contain the logarithmic term. The excitonic ground state energy in this case undergoes a simple first order shift,

$$\Delta E_{0\text{ren}} = -\frac{aqq'}{(\epsilon_1 + \epsilon_2)\rho_0}. \quad (33)$$

Notice that our renormalization procedure eliminates logarithmic terms in all orders of the *monopole* perturbation, not just the first one. For example, keeping the second order monopole contribution in square brackets in Eq. (26) would add the term

$$V_{2\text{ren}}^{(\text{monopole})} = \frac{3a^2}{16} \frac{\pi qq'}{(\epsilon_1 + \epsilon_2)\rho_0} \left[\frac{8}{\pi} b + b^2 Y_0(b) - b^2 H_0(b) + 3b Y_1(b) - 3b H_1(b) \right] \quad (34)$$

to the potential in (28), which in the $b \ll 1$ limit is just

$$V_{2\text{ren}}^{(\text{monopole})} = -\frac{9a^2}{8} \frac{qq'}{(\epsilon_1 + \epsilon_2)\rho_0}. \quad (35)$$

Returning to the linear approximation (28), we again define two relative errors,

$$\text{Err}_{1\text{ren}} \equiv \frac{V_{\text{exact}} - V_{\text{ren approx}}}{V_{\text{exact}}} = \frac{V_{1\text{ren exact}} - V_{1\text{ren}}}{V_{\text{exact}}}, \quad (36)$$

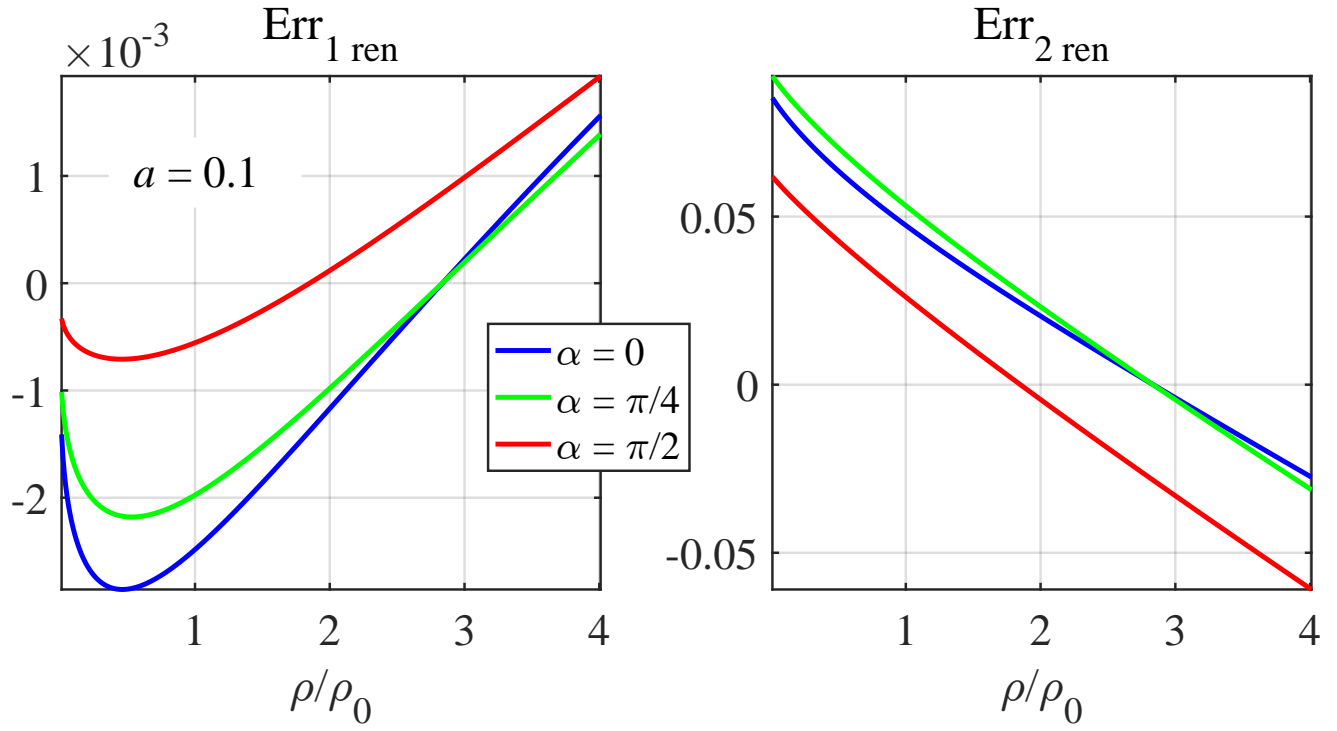


FIG. 4: Graphs of the relative errors defined in Eqs. (36) and (37). Compare with Fig. 2.

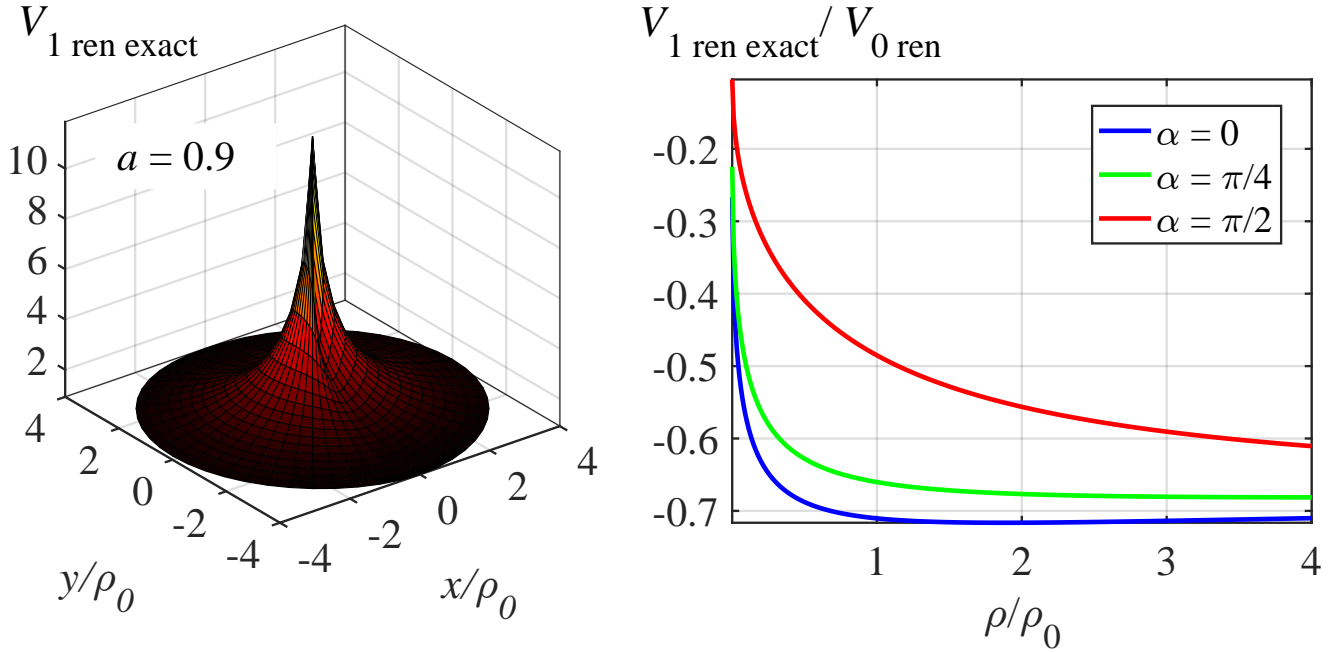


FIG. 5: Graphs of $V_{1 \text{ ren exact}}$ in units of $|qq'|/(\epsilon_1 + \epsilon_2)\rho_0$ and $V_{1 \text{ ren exact}}/V_{0 \text{ ren}}$, with $a = 0.9$, in the strongly anisotropic case (calculated numerically on the basis of Eqs. (10) and (29)).

and

$$\text{Err}_{2 \text{ ren}} \equiv \frac{V_{\text{exact}} - V_{\text{ren approx}}}{V_{\text{exact}} - V_{0 \text{ ren}}} = \frac{V_{1 \text{ ren exact}} - V_{1 \text{ ren}}}{V_{1 \text{ ren exact}}}, \quad (37)$$

with $V_{1\text{ren exact}} \equiv V_{\text{exact}} - V_{0\text{ren}}$ and $V_{\text{ren approx}} \equiv V_{0\text{ren}} + V_{1\text{ren}}$. The corresponding numerical results presented in Fig. 4 show that our revised approximation scheme is indeed superior to the one used in Sec. III.

Finally, we also performed numerical simulations in the extreme anisotropic regime, as shown in Fig. 5. In this case, the ‘‘correction’’ $V_{1\text{ren exact}}$ becomes comparable to $V_{0\text{ren}}$, and the linear approximation breaks down.

V. SUMMARY

The classic Keldysh-Rytova formula for screened Coulomb interaction in semiconductor thin films has been generalized by taking into account the anisotropy of the layer’s dielectric permittivity tensor. The Fourier image of the anisotropic potential in momentum space, as well as the linear correction to the isotropic potential in real space, have been worked out in closed analytical form. The case of strong in-plane anisotropy, however, remains unresolved due to the appearance of the function $I(t, \alpha, a, b)$ (see Eqs. (11) and (14)), whose explicit analytical expression is not known.

Acknowledgments

The author thanks Robert Zaballa for useful discussions.

APPENDIX: Momentum space representation

Following [16] and [17], we consider a geometry in which the anisotropic semiconductor film occupies the region of space $-d/2 \leq z \leq d/2$, as shown in Fig. 6. The half-space $z < -d/2$ (the substrate) is filled with an isotropic medium whose dielectric constant is ϵ_1 , while the half-space $z > d/2$ with an isotropic medium whose dielectric constant is ϵ_2 .

We are assuming that the axes of the coordinate system (x, y, z) coincide with the principal axes of the film’s dielectric permittivity tensor. The electrostatic potential at point $\mathbf{r} \equiv (\boldsymbol{\rho}, z) = (x, y, z)$ due to charge q' located at $\mathbf{r}' = (0, 0, z')$ satisfies in regions 1, 2, and 3 (the film) the following system of equations:

$$\left(\frac{\partial^2}{\partial x^2} + \frac{\partial^2}{\partial y^2} + \frac{\partial^2}{\partial z^2} \right) \phi_1(\mathbf{r}, \mathbf{r}') = 0, \quad (38)$$

$$\left(\frac{\partial^2}{\partial x^2} + \frac{\partial^2}{\partial y^2} + \frac{\partial^2}{\partial z^2} \right) \phi_2(\mathbf{r}, \mathbf{r}') = 0, \quad (39)$$

$$\left(\epsilon_x \frac{\partial^2}{\partial x^2} + \epsilon_y \frac{\partial^2}{\partial y^2} + \epsilon_z \frac{\partial^2}{\partial z^2} \right) \phi_3(\mathbf{r}, \mathbf{r}') = -4\pi q' \delta(\mathbf{r} - \mathbf{r}'), \quad (40)$$

with the boundary conditions at the interfaces,

$$(\phi_2 - \phi_3)_{z=\frac{d}{2}} = 0, \quad \left(\epsilon_2 \frac{\partial \phi_2}{\partial z} - \epsilon_z \frac{\partial \phi_3}{\partial z} \right)_{z=\frac{d}{2}} = 0, \quad (41)$$

$$(\phi_3 - \phi_1)_{z=-\frac{d}{2}} = 0, \quad \left(\epsilon_z \frac{\partial \phi_3}{\partial z} - \epsilon_1 \frac{\partial \phi_1}{\partial z} \right)_{z=-\frac{d}{2}} = 0, \quad (42)$$

and the boundary conditions at the two infinities,

$$\phi_2|_{z \rightarrow +\infty} = 0, \quad \phi_1|_{z \rightarrow -\infty} = 0. \quad (43)$$

Fourier transforming,

$$\phi_{1,2,3}(\mathbf{r}, \mathbf{r}') = \int \frac{d^2 \mathbf{k}}{(2\pi)^2} e^{i\mathbf{k} \cdot \boldsymbol{\rho}} \phi_{1,2,3}(\mathbf{k}, z, z'), \quad \mathbf{k} = (k_x, k_y), \quad (44)$$

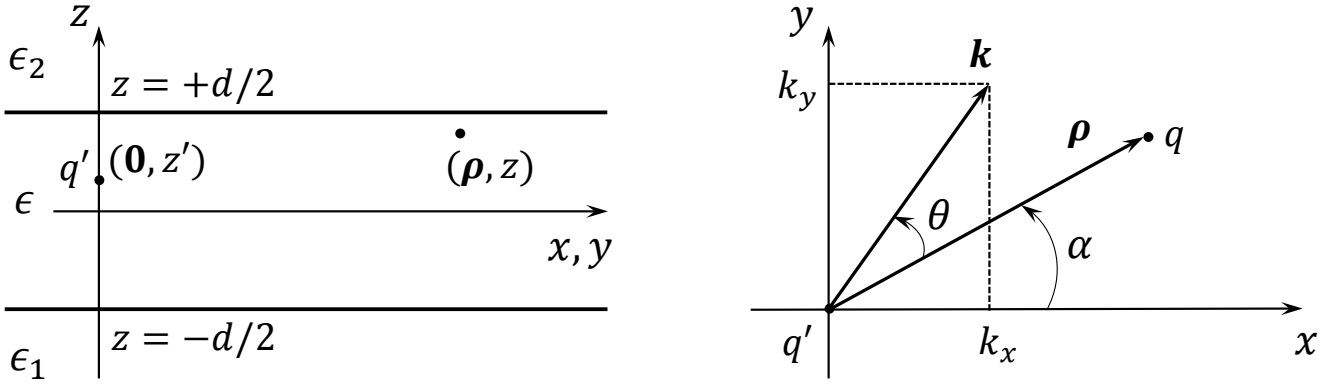


FIG. 6: Left: Semiconductor film geometry; the (x, y, z) axes coincide with the principal axes of the dielectric permittivity tensor of the film, ϵ . Right: Mutual orientation of vectors \mathbf{k} and $\boldsymbol{\rho}$ used in Eq. (5).

and substituting into (38), (39), and (40), we get the following equations for the corresponding Fourier components,

$$\left(\frac{\partial^2}{\partial z^2} - k^2\right) \phi_1(k, z, z') = 0, \quad (45)$$

$$\left(\frac{\partial^2}{\partial z^2} - k^2\right) \phi_2(k, z, z') = 0, \quad (46)$$

$$\left(\frac{\partial^2}{\partial z^2} - \tilde{k}^2\right) \phi_3(\tilde{k}, z, z') = -\frac{4\pi q'}{\epsilon_z} \delta(z - z'), \quad (47)$$

where

$$k \equiv |\mathbf{k}| = \sqrt{k_x^2 + k_y^2}, \quad \tilde{k} \equiv \sqrt{\frac{\epsilon_x k_x^2 + \epsilon_y k_y^2}{\epsilon_z}}. \quad (48)$$

Conditions at infinity, (43), combined with Eqs. (45) and (46) give

$$\phi_2(k) = A_2(z') e^{-kz}, \quad \frac{\partial \phi_2(k)}{\partial z} = -k A_2(z') e^{-kz}, \quad (49)$$

$$\phi_1(k) = A_1(z') e^{kz}, \quad \frac{\partial \phi_1(k)}{\partial z} = k A_1(z') e^{kz}, \quad (50)$$

while Eq. (47) gives, for $z \neq z'$,

$$\phi_3(\tilde{k}, z \neq z') = A_3(z') e^{\tilde{k}z} + B_3(z') e^{-\tilde{k}z}, \quad (51)$$

and, at $z = z'$, the jump discontinuity in the z -derivative,

$$\left. \frac{\partial \phi_3(\tilde{k})}{\partial z} \right|_{z=z'+0}^{z=z'-0} = -\frac{4\pi q'}{\epsilon_z}. \quad (52)$$

Imposing the boundary conditions at the $z = +d/2$ interface,

$$A_2(z') e^{-kd/2} = A_3(z') e^{\tilde{k}d/2} + B_3(z') e^{-\tilde{k}d/2}, \quad (53)$$

$$-\epsilon_2 k A_2(z') e^{-kd/2} = \epsilon_z \tilde{k} [A_3(z') e^{\tilde{k}d/2} - B_3(z') e^{-\tilde{k}d/2}], \quad (54)$$

we get

$$\phi_3(\tilde{k})|_{z > z'} = A_3(z') [e^{\tilde{k}z} + e^{2\tilde{\eta}_2 + \tilde{k}(d-z)}], \quad (55)$$

where

$$\tilde{\eta}_2 \equiv \frac{1}{2} \ln \left(\frac{\epsilon_z \tilde{k} + \epsilon_2 k}{\epsilon_z \tilde{k} - \epsilon_2 k} \right). \quad (56)$$

Similarly, imposing the boundary conditions at the $z = -d/2$ interface, we get

$$\tilde{A}_3(z')e^{-\tilde{k}d/2} + \tilde{B}_3(z')e^{\tilde{k}d/2} = A_1(z')e^{-kd/2}, \quad (57)$$

$$\epsilon_z \tilde{k} \left[\tilde{A}_3(z')e^{-\tilde{k}d/2} - \tilde{B}_3(z')e^{\tilde{k}d/2} \right] = \epsilon_1 k A_1(z')e^{-kd/2}, \quad (58)$$

and, after defining

$$\tilde{\eta}_1 \equiv \frac{1}{2} \ln \left(\frac{\epsilon_z \tilde{k} + \epsilon_1 k}{\epsilon_z \tilde{k} - \epsilon_1 k} \right), \quad (59)$$

find

$$\phi_3(\tilde{k})|_{z < z'} = \tilde{A}_3(z') \left[e^{\tilde{k}z} + e^{-2\tilde{\eta}_1 - \tilde{k}(d+z)} \right]. \quad (60)$$

Now, for $z = z'$, Eqs. (52), (55), and (60) give

$$A_3(z') \left[e^{\tilde{k}z'} + e^{2\tilde{\eta}_2 + \tilde{k}(d-z')} \right] - \tilde{A}_3(z') \left[e^{\tilde{k}z'} + e^{-2\tilde{\eta}_1 - \tilde{k}(d+z')} \right] = 0, \quad (61)$$

$$\tilde{k} A_3(z') \left[e^{\tilde{k}z'} - e^{2\tilde{\eta}_2 + \tilde{k}(d-z')} \right] - \tilde{k} \tilde{A}_3(z') \left[e^{\tilde{k}z'} - e^{-2\tilde{\eta}_1 - \tilde{k}(d+z')} \right] = -\frac{4\pi q'}{\epsilon_z}, \quad (62)$$

resulting in

$$\tilde{A}_3(z') = A_3(z') \frac{e^{\tilde{k}z'} + e^{2\tilde{\eta}_2 + \tilde{k}(d-z')}}{e^{\tilde{k}z'} + e^{-2\tilde{\eta}_1 - \tilde{k}(d+z')}}}, \quad (63)$$

and

$$A_3(z') = \frac{4\pi q' e^{-\tilde{k}d/2 - \tilde{\eta}_2} \cosh \left[\tilde{k}(d/2 + z') + \tilde{\eta}_1 \right]}{\epsilon_z \tilde{k} 2 \sinh \left[\tilde{k}d + \tilde{\eta}_1 + \tilde{\eta}_2 \right]}. \quad (64)$$

Taking into account that

$$e^{\tilde{k}z} + e^{2\tilde{\eta}_2 + \tilde{k}(d-z)} = 2e^{\tilde{k}d/2 + \tilde{\eta}_2} \cosh \left[\tilde{k}(d/2 - z) + \tilde{\eta}_2 \right], \quad (65)$$

we get

$$\phi_3(\tilde{k}, z > z') = \frac{4\pi q' \cosh \left[\tilde{k} \left(\frac{d}{2} - z \right) + \tilde{\eta}_2 \right] \cosh \left[\tilde{k} \left(\frac{d}{2} + z' \right) + \tilde{\eta}_1 \right]}{\epsilon_z \tilde{k} \sinh \left[\tilde{k}d + \tilde{\eta}_1 + \tilde{\eta}_2 \right]}. \quad (66)$$

For $z < z'$, a similar calculation results in

$$\phi_3(\tilde{k}, z < z') = \frac{4\pi q' \cosh \left[\tilde{k} \left(\frac{d}{2} - z' \right) + \tilde{\eta}_2 \right] \cosh \left[\tilde{k} \left(\frac{d}{2} + z \right) + \tilde{\eta}_1 \right]}{\epsilon_z \tilde{k} \sinh \left[\tilde{k}d + \tilde{\eta}_1 + \tilde{\eta}_2 \right]}. \quad (67)$$

[1] P. Cudazzo, C. Attaccalite, I. V. Tokatly, and A. Rubio, “Strong Charge-Transfer Excitonic Effects and the Bose-Einstein Exciton Condensate in Graphane,” *Phys. Rev. Lett.* **104**, 226804 (2010).

- [2] P. Cudazzo, I. V. Tokatly, and A. Rubio, “Dielectric screening in two-dimensional insulators: Implications for excitonic and impurity states in graphane,” *Phys. Rev. B* **84**, 085406 (2011).
- [3] A. Chernikov, T. C. Berkelbach, H. M. Hill, A. Rigosi, Y. Li, O. B. Aslan, D. R. Reichman, M. S. Hybertsen, and T. F. Heinz, “Exciton Binding Energy and Nonhydrogenic Rydberg Series in Monolayer WS_2 ,” *Phys. Rev. Lett.* **113**, 076802 (2014).
- [4] T. Low, R. Roldán, H. Wang, F. Xia, P. Avouris, L. M. Moreno, and F. Guinea, “Plasmons and Screening in Monolayer and Multilayer Black Phosphorus,” *Phys. Rev. Lett.* **113**, 106802 (2014).
- [5] X. Wang, A. M. Jones, K. L. Seyler, V. Tran, Y. Jia, H. Zhao, H. Wang, L. Yang, X. Xu and F. Xia, “Highly anisotropic and robust excitons in monolayer black phosphorus,” *Nature Nanotechnology* **10**, 517 (2015).
- [6] A. Chaves, T. Low, P. Avouris, D. Cakir, and F. M. Peeters, “Anisotropic exciton Stark shift in black phosphorus,” *Phys. Rev. B* **92**, 155311 (2015).
- [7] S. Latini, T. Olsen, and K. S. Thygesen, “Excitons in van der Waals heterostructures: The important role of dielectric screening,” *Phys. Rev. B* **92**, 245123 (2015).
- [8] T. G. Pedersen, S. Latini, K. S. Thygesen, H. Mera and B. K. Nikolić, “Exciton ionization in multilayer transition-metal dichalcogenides,” *New J. Phys.* **18** (2016).
- [9] M. L. Trolle, T. G. Pedersen and V. Véniard, “Model dielectric function for 2D semiconductors including substrate screening,” *Nature Sci. Rep.* **7**, 39844 (2017).
- [10] A. Hichri, I. B. Amara, S. Ayari and S. Jaziri, “Dielectric environment and/or random disorder effects on free, charged and localized excitonic states in monolayer WS_2 ,” *J. Phys.: Condens. Matter* **29**, 435305 (2017).
- [11] M. Szyniszewski, E. Mostaani, N. D. Drummond, and V. I. Falko, “Binding energies of trions and biexcitons in two-dimensional semiconductors from diffusion quantum Monte Carlo calculations,” *Phys. Rev. B* **95**, 081301(R) (2017).
- [12] E. Mostaani, M. Szyniszewski, C. H. Price, R. Maezono, M. Danovich, R. J. Hunt, N. D. Drummond, V. I. Falko, “Diffusion quantum Monte Carlo study of excitonic complexes in two-dimensional transition-metal dichalcogenides,” *Phys. Rev. B* **96**, 075431(2017).
- [13] L. S. R. Cavalcante, A. Chaves, B. Van Duppen, F. M. Peeters, and D. R. Reichman, “Electrostatics of electron-hole interactions in van derWaals heterostructures,” *Phys. Rev. B* **97**, 125427 (2018).
- [14] Sh. Niu, G. Joe, H. Zhao, Y. Zhou, T. Orvis, H. Huyan, J. Salman, K. Mahalingam, B. Urwin, J. Wu, Y. Liu, T. E. Tiwald, S. B. Cronin, B. M. Howe, M. Mecklenburg, R. Haiges, D. J. Singh, H. Wang, M. A. Kats and J. Ravichandran, “Giant optical anisotropy in a quasi-one-dimensional crystal,” *Nature Photonics* **12**, 392 (2018).
- [15] Sh. Niu, H. Zhao, Y. Zhou, H. Huyan, B. Zhao, J. Wu, S. B. Cronin, H. Wang, and J. Ravichandran, “Mid-wave and Long-Wave Infrared Linear Dichroism in a Hexagonal Perovskite Chalcogenide,” *Chem. Mater.* **30** (15), 4897 (2018).
- [16] N. S. Rytova, “Screened potential of a point charge in a thin film,” *Vestn. Mosk. Univ. Fiz. Astron.* **3**, 30 (1967).
- [17] L. V. Keldysh, “Coulomb interaction in thin semiconductor and semimetal films,” *Pis'ma Zh. Eksp. Teor. Fiz.* **29**, 716 (1979) [*JETP Lett.*, **29**, 658 (1979)].
- [18] L. V. Keldysh, “Excitons in Semiconductor-Dielectric Nanostructures,” *Phys. Stat. Sol. (a)* **164**, 3 (1997).
- [19] T. C. Berkelbach, M. S. Hybertsen, D. R. Reichman, “Theory of neutral and charged excitons in monolayer transition metal dichalcogenides,” *Phys. Rev. B* **88**, 045318 (2013).
- [20] S. G. Mikhlín, *Integral Equations*, Second Revised Edition (Pergamon Press, 1964).